

Article

Self-Sustainability Assessment for a High Building Based on Linear Programming and Computational Fluid Dynamics

Carlos Oliveira ¹, José Baptista ^{1,*} and Adelaide Cerveira ²

¹ Departamento de Engenharias, Escola de Ciências e Tecnologia, Universidade de Trás-os-Montes, e INESC-TEC UTAD Pole, 5000-801 Vila Real, Portugal

² Departamento de Matemática, Escola de Ciências e Tecnologia, Universidade de Trás-os-Montes, e INESC-TEC UTAD Pole, 5000-801 Vila Real, Portugal

* Correspondence: baptista@utad.pt

Abstract: With excess energy use from non-renewable sources, new energy generation solutions must be adopted to make up for this excess. In this sense, the integration of renewable energy sources in high-rise buildings reduces the need for energy from the national power grid to maximize the self-sustainability of common services. Moreover, self-consumption in low-voltage and medium-voltage networks strongly facilitates a reduction in external energy dependence. For consumers, the benefits of installing small wind turbines and energy storage systems include tax benefits and reduced electricity bills as well as a profitable system after the payback period. This paper focuses on assessing the wind potential in a high-rise building through computational fluid dynamics (CFD) simulations, quantifying the potential for wind energy production by small wind turbines (WT) at the installation site. Furthermore, a mathematical model is proposed to optimize wind energy production for a self-consumption system to minimize the total cost of energy purchased from the grid, maximizing the return on investment. The potential of a CFD-based project practice that has wide application in developing the most varied processes and equipment results in a huge reduction in the time and costs spent compared to conventional practices. Furthermore, the optimization model guarantees a significant decrease in the energy purchased at peak hours through the energy stored in energy storage systems (ESS). The results show that the efficiency of the proposed model leads to an investment amortization period of 7 years for a lifetime of 20 years.

Keywords: distributed energy resources; small wind turbine; optimization; mixed-integer linear programming; computational fluid dynamics; self-consumption



check for updates

Citation: Oliveira, C.; Baptista, J.; Cerveira, A. Self-Sustainability Assessment for a High Building Based on Linear Programming and Computational Fluid Dynamics. *Algorithms* **2023**, *16*, 107. <https://doi.org/10.3390/a16020107>

Academic Editor: Abdulsalam Yassine

Received: 7 December 2022

Revised: 27 January 2023

Accepted: 4 February 2023

Published: 13 February 2023



Copyright: © 2023 by the authors. Licensee MDPI, Basel, Switzerland. This article is an open access article distributed under the terms and conditions of the Creative Commons Attribution (CC BY) license (<https://creativecommons.org/licenses/by/4.0/>).

1. Introduction

Population growth in urban areas has triggered the search for sustainable techniques of energy consumption in buildings [1–3]. It is necessary to prioritize energy efficiency and integrate renewable energy sources in buildings to achieve EU goals [4]. Buildings are responsible for 40% of the total energy consumption across the EU, and the share of energy-inefficient buildings is 36%, mainly due to their age, which is over 50 years [5–7]. Energy management in buildings is associated with the idea of controlling different energy sources and loads in an efficient and optimized manner with one purpose: to reduce energy costs by measuring the energy demand of the load and the production of renewable energy sources locally in real time [8,9].

On-site energy generation has several advantages not only in environmental terms but also in economic and technological terms, such as reducing energy losses in the power grid and enhancing the autonomy and decision-making power of individual consumers, leading to a decrease in the balance of energy imports [10,11]. The integration of wind systems in urban environments must consider the maximization of renewable energy generation in cities and minimize negative impacts on health and the local environment

to ensure the essential energy needs of all those who live and work in these areas [12]. Distributed power production in urban areas is a remarkable contribution to the design of new sustainable buildings concerning energy consumption, produced directly where the energy demand is sought [13]. In addition to this growing interest in installing local generation in cities, small wind turbines also gain a focus of interest in the understanding of their potential in an urban environment [14]. Local electricity generation in buildings by wind turbines (WT) involves many different challenges in comparison to stand-alone wind energy systems and wind farms. It is known that the wind profile in an urban environment is very complex, and the adaptability of wind turbines to this environment is not sufficiently known, neither in terms of productivity nor in terms of compatibility with the building's structure. The high terrain roughness length and the presence of obstacles with different shapes strongly influence the air stream for wind power use. However, disturbed flows around buildings can locally increase wind speed, and energy yield can be increased in comparison to open locations. As the energy efficiency of WTs depends on the cubed wind speed, an increase in wind speed due to the surrounding buildings can make the turbines favourable to the wind [12–14].

Small wind turbines integrated into buildings are low-cost renewable energy sources Stankovic2009. Despite their potential, Ledo and co-authors Ledo2011 pointed out that the reasons for the limited installation of micro wind turbines in urban areas are the low average wind speed in these areas, the high levels of turbulence, and the relatively high levels of aerodynamics noise caused by the turbines. Blackmore [15,16] noted that if a turbine is installed in the wrong location on the roof of a building, power can drop to zero for significant periods, even when wind speeds are relatively favourable for energy production. The effort to optimize flow simulation models for different species should be valued. The potential of a CFD-based design practice that has wide application in developing the most varied processes and equipment results in a huge reduction in costs and expenses compared to conventional practices [17]. In addition, to achieve great efficiency in the use of energy in buildings, the integration of renewable energy sources in an optimized manner is crucial [6]. Several publications have proposed different approaches and methods related to the adoption, ideal design and control of energy consumption for new buildings, the ideal renovation or retrofit of existing buildings, and the ideal dimensioning of different RES, which are objectives to decrease the demand for energy and increase their efficiency [5,18–20].

This paper analyses and evaluates the energetic suitability of wind turbines to be installed on the rooftop of a building. It is important to numerically evaluate the influence on the air stream from buildings and rooftops and to model wind flows over buildings and their roofs to better design and install WTs based on local wind meteorological data and local urban terrain characteristics for assessing and improving local urban wind power production. The main objective of this research work is to assess the impact that integrated wind production in high-rise buildings can have on the economic sustainability of the consumption inherent in the management of the building itself. To this end, it is important to know the load diagrams involved in this process, the study of low-power wind technologies already on the market for application in this type of building, and which solutions best fit your needs. To minimize the consumption of energy to the grid, a linear programming (LP) optimization model was developed to optimize the self-consumption system, minimizing the total costs that include the costs of installing the turbines and batteries, as well as the cost of energy purchased from the distributor. Several case studies are considered, where the economic feasibility study will be investigated, and simulations will be carried out with the proposed optimization model.

This paper is organized as follows. Section 2 characterizes the study area and the adopted methodology; Section 2.1 addresses and characterizes the studied scenarios and refers to the data processing; Section 2.2 describes the scenarios for the CFD simulations and briefly how they were built; Section 2.3 presents a mixed-integer linear programming model to optimize the wind energy production for a self-consumption system to minimize the total

cost of energy purchased from the grid, maximizing the return on investment; Section 3 presents the results of the case studies about two roof formats; and finally, Section 4 draws the main conclusions.

2. Materials and Methods

This section briefly explains the methods used to carry out the proposed work, identifying the wind turbines best suited to the installation site, the possible locations for installing them through computational fluid analysis, and the mathematical optimization model.

2.1. Data and Procedures

The data to analyse the local wind profile and building energy consumption were collected throughout the whole year of 2019. Wind data were collected over a 10 min sampling period at a height of 30 m. Regarding the energy consumed, to build the load profile, the data were collected with a sampling period of 60 min.

Through the annual recording of the wind direction and speed, the graph in Figure 1, known as the wind rose, was obtained. One can observe the relative frequency of the wind speed range for the different wind directions that it can take. It can be highlighted that, in this case, the predominant wind directions are between 300 and 360 degrees, with the most predominant being 330 degrees, that is, from north-west to south-east.

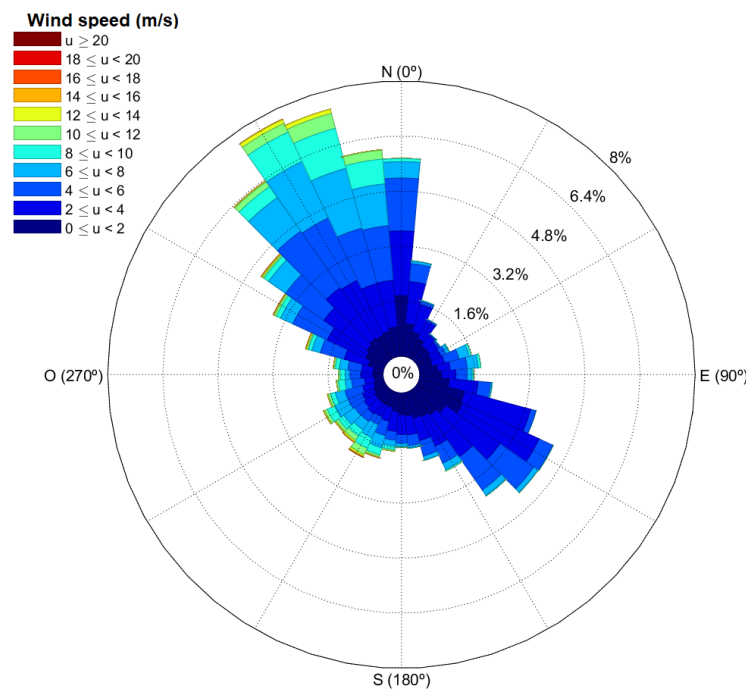


Figure 1. Wind rose for the case study adopted.

Table 1 summarizes the statistical measurements of the wind speed (u), such as mean (\bar{u}), median (Med), maximum, minimum, and sample standard deviation (s) for the record height (30 m) and extrapolated heights, 72 and 77 m. The speed extrapolation is performed by the application of the logarithmic law presented in (1) for each record collected. Comparing the average speed at 72 and 77 m with the reference speed at 30 m, an increase of 25–27% is observed, which corresponds to 1.05 m/s.

$$\bar{u}(z) = \frac{u_a}{k} \ln \frac{z}{z_0} \quad (1)$$

where $\bar{u}(z)$ is the average value of the wind speed at height z , u_a is the so-called friction speed, k represents the Von Karman constant whose value is equal to 0.4, and finally, z_0 defines the characteristic length of the roughness of the soil.

Table 1. Statistical measures of wind speed at different heights.

Height (m)	\bar{u}	Maximum	Minimum	Med	s
30	4.08	19.90	0.00	3.59	2.61
72	5.13	25.02	0.00	4.52	3.28
77	5.21	25.42	0.00	4.59	3.34

The wind speed directly influences the output power of wind turbines, which also depends on their technical specifications. This work considers two types of wind turbines, the Aeolos-V 10 kW and the Aeolos-H 20 kW [21]. To estimate the average annual load profile with the extrapolated calculations from the collected wind data, the power curves [21] from the wind turbines are needed. Figure 2 shows the power curve graph built from the information given by the wind turbine manufacturer. Extrapolated values have been rounded round off by default. Subsequently, a direct association was made between the extrapolated wind speed values and the turbine power curves. The power curve records the turbine power with an accuracy of 1 m/s.

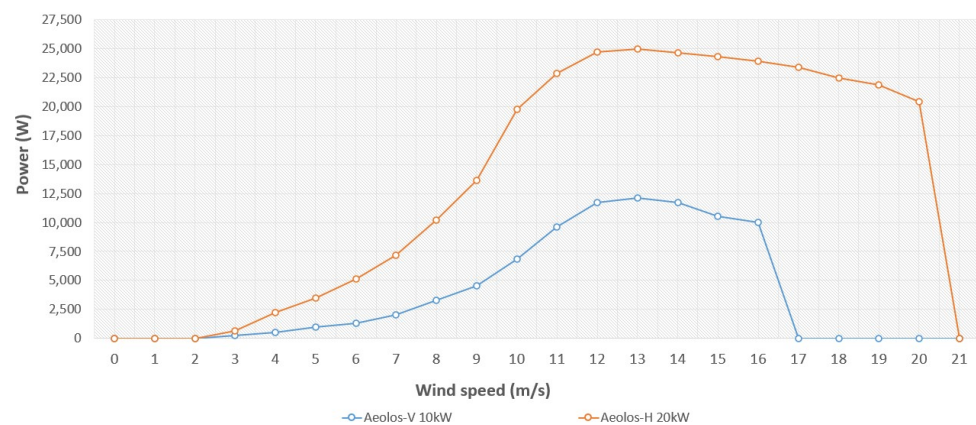


Figure 2. Turbine power curves.

The power available in the wind depends on the kinetic energy associated with an air column moving at speed u (m/s) and can be calculated using Equation (2).

$$P_{wind} = \frac{1}{2}(\rho Au)u^2 = \frac{1}{2}\rho Au^3 \tag{2}$$

where P_{wind} is the power available in the wind (in W), A is the rotor blade sweep area (m²), u is the wind speed (m/s), and ρ is the air density, usually considered constant during the year, the standard value being equal to 1.225 kg/m³. Equation (2) shows that the available power greatly depends on wind speed. Wind power cannot be fully converted into mechanical power in the turbine because, by Betz’s law, it is at most 59.3% [22] of the kinetic energy that it converted into mechanical energy to be used in the turbine.

Knowing the wind profile and the turbine power curve, it is possible to determine the energy produced during a period for a single wind direction using Equation (3).

$$PW = T \int_{u_0}^{u_\infty} P_e(u) f_w(u) du \tag{3}$$

where E is the annual energy produced (kWh), T is the number of hours during the considered period, f_w is the Weibull probability density function, and $P_e(u)$ is WT power (kW) for u wind speed [23].

2.2. Study Area Characterisation

The studied area is characterized by being a relatively flat area without any obstacles to the west, as the building is quite close to the beach.

In Figure 3, a portion of the urbanization of the study area with six buildings in total is presented. The study building, represented by H, is surrounded by five buildings of different sizes and shapes, except for its western orientation zone. First, a three-dimensional drawing was made to be inserted into the software where the computational fluid simulations would be executed.

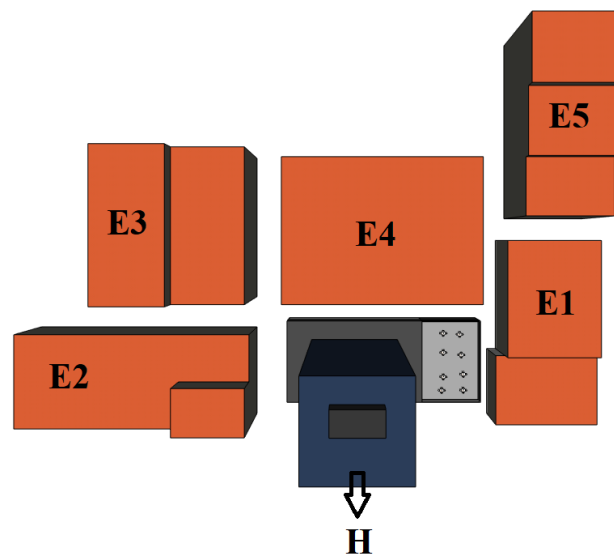


Figure 3. Top view of the tridimensional model.

The most relevant characteristics concerning the buildings are presented in Table 2, where the dimensions of the buildings are presented in meters for the x , y , and z plane, with z being the height.

Table 2. Dimensions of the buildings of the study area.

Building Identification	Dimensions (x, y, z) (m)	Total Coverage Area (m^2)
H	19, 17, 72	323
E1	20, 40, 19	800
E2	50, 20, 30	1000
E3	30, 32, 37	960
E4	41, 30, 30	1230
E5	18, 40, 37	720

Figure 4 shows the average annual load profile, built from the available energy consumption data. A brief analysis of the load profile shows that the hours of the day with the highest consumption, between 22,500 kWh to 26,500 kWh, are in the early morning, from 7:00 to 9:00, and in the late afternoon, from 18:00 to 21:00.

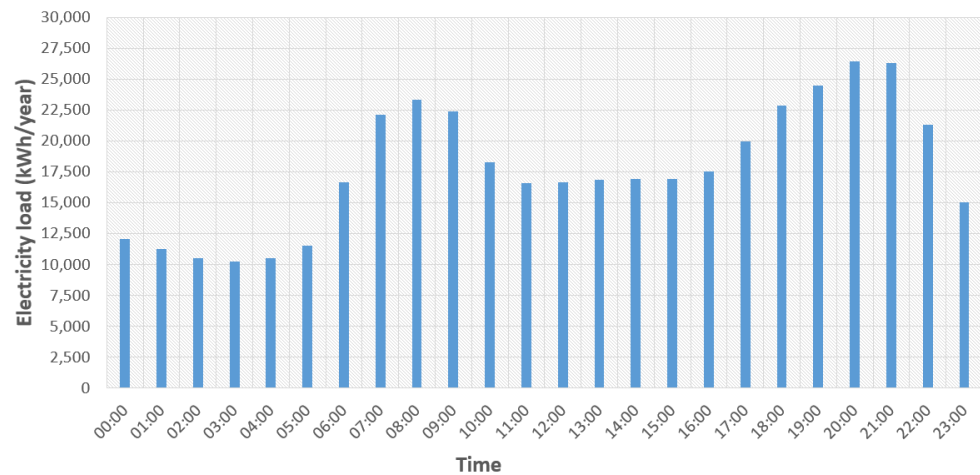


Figure 4. Building load profile.

2.3. Optimization Model

Energy optimization in buildings through mathematical optimization has sparked academic interest in recent years. In this paper, a mixed-integer linear programming model is proposed to minimize energy-related costs, considering day-ahead market prices and storage limitations, as well as RES demand and generation profiles.

The data for this problem are the building's electricity demand, the wind energy production for both scenarios described here, and the cost of electricity for both normal and optional tariffs.

This problem is modelled for a period of 20 years, which is the expected period of a turbine's useful life according to the turbine's manufacturer. It will also be the period to analyse the financial return of the investment made for each scenario. Besides the turbines, it is also possible to install energy storage systems (ESS) to store surplus wind power or store energy purchased from the power grid in more convenient periods to be used in the future. In the event that the installation of ESS in the building is profitable, each scenario takes into account its lifetime (pb). That is, for the period of financial analysis, the replacement of new batteries according to their lifetime is taken into account.

2.3.1. Data Sets and Parameters

The data for the optimization problem is described below:

- $P = \{1, \dots, n_p\}$, the set of 15 min periods for one year with $n_p = 8760$;
- $T = \{1, 2\}$, the set of available tariffs (1—normal; 2—optional);
- $WT = \{1, 2\}$, the set of wind turbines;
- $B = \{1, 2\}$, the set of batteries that can be used;
- pb , battery lifetime in years ($pb \in \{5, 10, 15, 20\}$);
- $c(i, j)$, price (EUR/kWh) in period i adopting the tariff j , $i, j \in P, T$;
- $pw(i, j)$, energy production (kWh) in period i using the turbine j , $i \in P, j \in WT$;
- $d(i)$, energy demand (kWh) in period i , $i \in P$.
- $M = \sum_{i \in P} d(i)$, increased value representing the sum of the energy demand values;
- $kb(i)$, capacity of the battery i (kW), $i \in B$;
- $cb(i)$, cost of the battery i in Euros, $i \in B$;
- $cWT(j)$, cost of wind turbine j , $j \in WT$;
- $rr = 0.02$, inflation rate of the energy price purchased from the grid.

In Table 3, are presented some details regarding the wind turbine set, and Table 4 presents some details regarding the batteries set.

Table 3. Description of wind turbine set: designation and unit cost.

Data	Wind Turbine Set, WT	
	1	2
Name	Aeolos-V 10 kW	Aeolos-H 20 kW
c_{WT}	18,364.15 EUR	26,589.08 EUR

Table 4. Description of battery set: designation, unit cost, and capacity.

Data	Battery Set, B	
	1	2
Name	LG Resu13	BYD LVS 8.0
cb	5679 EUR	3815 EUR
kb	12.4 kWh	8.0 kWh

Regarding the cost of electricity from the grid, there is a price adjustment each year, also known as the energy price inflation rate. For this study, the energy price inflation rate was adopted as 2% per year, represented by e , according to [24]. Equation (4) determines the energy cost for each period and year.

$$POE_i = POE_0 \cdot (1 + e)^i \tag{4}$$

2.3.2. Decision Variables

The decision variables are:

- $x(i, j)$, energy (kWh) that is bought to the grid in period i by adopting the tariff j , $i \in P, j \in T$;
- $v(i)$, number of used batteries of type i , $i \in B$;
- $ab(i)$, power (kW) stored in the battery during the period i , $i \in P$;
- $db(i)$, battery power supply (kW) during the period i , $i \in P$;
- $s(i)$, stock of energy (kWh) in the battery at the beginning of the period i , $i \in P$;
- $y(j)$, binary variable that assumes the value 1 if turbine type j is used and assumes the value 0 otherwise, $j \in WT$;
- $w(j)$, binary variable that assumes value 1 if is adopted the tariff j , and assumes the value 0 otherwise, $j \in T$;
- $bb(j)$, binary variable that assumes the value 1 if the storage system j is used and assumes the value 0 otherwise, $j \in B$;
- $z(i)$, binary variable that indicates whether the energy stored in the batteries is used in the period i , $i \in P$;
- $zz(i)$, binary variable that indicates whether there is energy storage in the batteries in the period i , $i \in P$.

2.3.3. Mathematical Formulation

The mixed-integer linear programming model that minimizes energy and investment costs, and ensures that the demand is met, is given by (5)–(27).

$$\min \sum_{j \in T} c_{WT}(j) \cdot y(j) + \sum_{\ell \in B} c_b(\ell) \cdot v(\ell) + \sum_{t=1}^{pb} \sum_{i \in P} \sum_{j \in T} (x(i, j) \cdot c(i, j) \cdot (1 + rr)^{t-1}) \tag{5}$$

$$\text{s.t. } \sum_{j \in T} w(j) = 1 \tag{6}$$

$$\sum_{j \in WT} y(j) \leq 1 \tag{7}$$

$$\sum_{j \in B} bb(j) \leq 1 \tag{8}$$

The objective function (5) represents the total cost of investment in wind turbines and batteries along with the value of energy purchased from the grid for the adopted period. Constraint (6) forces the choice of a tariff for the purchase of energy for the building. Constraints (7) and (8) prevent the choice of more than one type of turbine or battery.

$$s(i) \leq \sum_{j \in B} kb(j) \cdot v(j), i \in P \tag{9}$$

$$db(i) \leq s(i), i \in P \tag{10}$$

$$ab(i) \leq \sum_{j \in B} kb(j) \cdot v(j), i \in P \tag{11}$$

$$s(i + 1) = s(i) + ab(i) - db(i), i \in 1 \dots np - 1 \tag{12}$$

The constraints (9)–(12) check the conditions for charging, discharging, and stocking the batteries, so that the operation of the energy storage system works correctly.

$$db(i) + \sum_{j \in T} x(i, j) + \sum_{\ell \in WT} pw(i, \ell) \cdot y(\ell) = d(i) + ab(i), i \in P \tag{13}$$

Constraints (13) ensure that, for all periods, the energy demand is met and the power surplus is stored. It provides that all the energy used from the batteries with the energy purchased from the power grid and the energy produced by the wind turbines is equal to the demand plus the energy stored in the batteries.

$$db(i) \leq Mb \cdot z(i), i \in P \tag{14}$$

$$z(i) \leq db(i), i \in P \tag{15}$$

$$ab(i) \leq Mb \cdot zz(i), i \in P \tag{16}$$

$$zz(i) \leq ab(i), i \in P \tag{17}$$

$$z(i) + zz(i) \leq 1, i \in P \tag{18}$$

Regarding the binary variables of charge/discharge of the ESS, constraints (14)–(18) prevent a charge and discharge from happening simultaneously. According to constraints (14) and (15), if there is a discharge from a battery in a period $i \in P$, $z(i)$ assumes value 1; otherwise, it assumes a value of 0. If there is a charge, $zz(i)$ assumes the value 1, according to the constraints (16) and (17). Constraint (18) prevents that the binary variables of charge and discharge having values of 1 at the same period $i \in P$.

$$\sum_{i \in P} x(i, j) \leq M \cdot w(j), j \in T \tag{19}$$

$$w(j) \leq \sum_{i \in P} x(i, j), j \in T \tag{20}$$

$$v(j) \leq Mv \cdot bb(j), j \in B \tag{21}$$

$$bb(j) \leq v(j), j \in B \quad (22)$$

Constraints (19) and (20) prevent more than one tariff $j \in T$ from being used, whereas constraints (21) and (22) restrain the use of more than one type of ESS, $j \in B$, in the model.

$$\sum_{i \in P} zz(i) \cdot pb \leq cycles \quad (23)$$

Constraint (23) ensures that the charge and discharge cycles of the batteries that limit the battery's life, in this case, $cycles = 6000$, are not exceeded.

$$x(i, j) \geq 0, i \in P, j \in T \quad (24)$$

$$v(i) \in Z, i \in B \quad (25)$$

$$ab(i), db(i), s(i) \geq 0, i \in P \quad (26)$$

$$z(i), zz(i), w(j), y(i), bb(\ell) \in \{0, 1\}, j \in T, i \in WT, \ell \in B \quad (27)$$

Constraints (24)–(27) establish the domain of the variables.

3. Results and Discussion

This section presents and discusses the results obtained using Ansys Fluent for the computational fluids dynamic and by solving the optimization model. As a result, it will be possible to analyse the different scenario results obtained to ascertain the optimal solution for the building.

3.1. CFD Results

It is intended to evaluate the modifications induced by the elements of the building's surroundings of an area with heterogeneous morphological characteristics to identify the places with more favourable conditions for the use of wind energy.

The geometric model for the CFD simulation was designed in the CFD simulation software itself (Ansys Fluent). The enclosure has the north wall of the volume as the fluid entry zone, which corresponds to the zone where the wind direction is more predominant. The enclosure fluid outlet zones correspond to the remaining sides of the enclosure, with the exception of the base, which is considered to be a wall. The buildings were characterized as contact regions, and in this way, they can influence the movement profile of the fluid, in this case, the air. To compute the geometric model, an automatic mesh from the Fluent workbench was parametrised with smooth transitions, five layers of inflation, and a medium relevance centre. In total, 65,390 nodes and 362,172 elements were computed. The fluid was defined as air, with a reference density of 1225 kg/cm^3 and an initial velocity in the volume (inlet) of 5 m/s .

The supposed location of installation of the turbines is not affected by changes in the wind direction or wind speed from other buildings. It appears that the airflow from north to south increases. It goes from 5 m/s to about 6.8 to 7.8 m/s , representing an increase from 36% to 58%. The airflow behaviour can be seen in Figure 5.

In this case, we can say that the shallow turbulence at the top of the building would not influence a turbine installed on the block above the top of the building. Through Figure 6, it can be seen that at the top of the building, the wind speed changes. There is a decrease to practically 0 m/s in the central and lateral zones, except for the block that is at the top.

The block on the hotel's roof would be an excellent place to install any of the turbines adopted for the case study. Furthermore, the north corners of the top are a perfect area for vertical axis turbines, as they are unidirectional turbines. Hence, if the turbine to be

installed is turbine 1, Aeolos-V 10 kW, the best proposal would be the installation of two of them in both north corners of the roof marked with an “X” in Figure 7. Alternatively, turbine 2, Aeolos-H 20 kW, would be installed on top of the block above the hotel marked with a dot in Figure 7. There is also the possibility of installing the vertical axis turbine at the top of the block. However, the difference observed in the production between the two turbines, 1 and 2, for the same height leads to discarding this option.

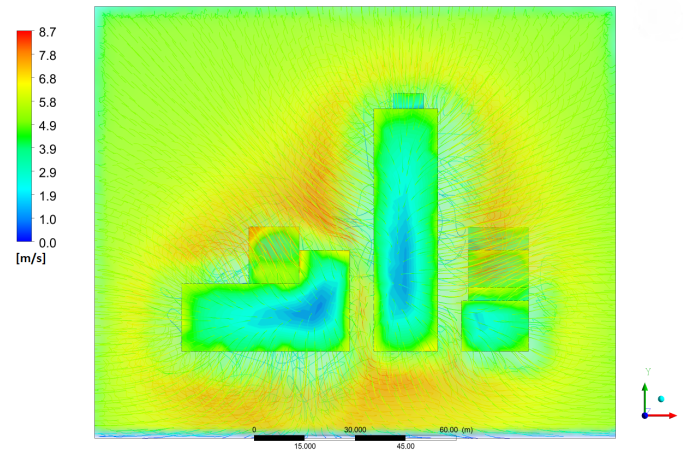


Figure 5. Speed contours in the north–south plane in the flow of air through buildings.

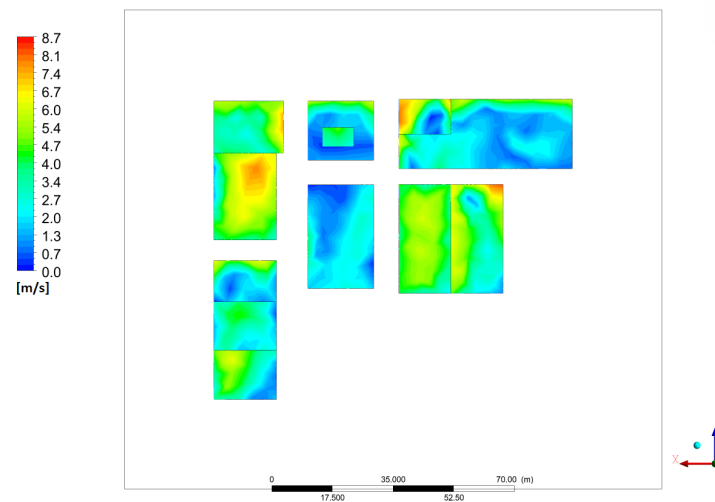


Figure 6. Top view of wind speed at the top of buildings.

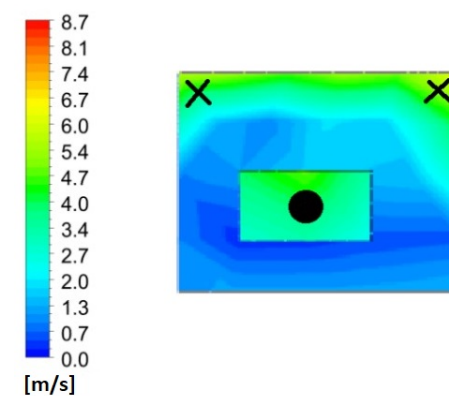


Figure 7. Scenario identification for the installation of wind turbines in the building’s rooftop.

3.2. Optimal Solutions for the LP Optimization Model

Tests were carried out for the 20 years of average wind turbine life for each possible scenario concerning the battery lifetime, *pb*. Scenarios 1, 2, 3, and 4 correspond, respectively, to the battery life, *pb*, equal to 5, 10, 15, and 20 years. For scenarios 1, 2, 3, and 4, the ESS was replaced 3, 2, 1, and 0 times, respectively. In this way, if possible, the LP model will determine four optimal solutions, one for each scenario. The results are presented in Table 5. It is easily identified which turbine and the tariff to be adopted for each scenario and the number of batteries used for the 20 years period.

Table 5. Optimal solutions for each scenario.

	Scenario 1	Scenario 2	Scenario 3	Scenario 4
Optimal value	221,023.49 EUR	431,492.59 EUR	663,920.59 EUR	920,959.21 EUR
Tariff	Optional tariff	Optional tariff	Optional tariff	Optional tariff
Wind turbine	Aeolos-H 20 kW	Aeolos-H 20 kW	Aeolos-H 20 kW	Aeolos-H 20 kW
Battery	BYD 8 kW	BYD 8 kW	BYD 8 kW	LG Resu 13 kW
N. of batteries	4	3	2	1

In either scenario, the optimal solution corresponds to the use of the horizontal axis turbine, Aeolos-H 20 kW, and the optional tariff. These are the choices that guarantee the best performance to the problem created. Concerning the batteries, there is a consensus on adopting the 8 kWh battery for scenarios 1, 2, and 3. However, for scenario 4 it is more profitable to adopt the 13 kWh battery.

Figure 8 shows the original real load profile for the building under study, represented by the black bar, together with the load profile's obtained with the optimization of energy purchased from the grid and necessary investments.

There was a considerable reduction in the energy purchase from the grid from 14:00 to 21:00. According to the legal summer or wintertime, this period can correspond to peak or full time. The period with the most significant reduction in the energy purchase from the grid was 17:00 h, where the purchase of energy suffered a reduction between 18.16% and 20.45%.

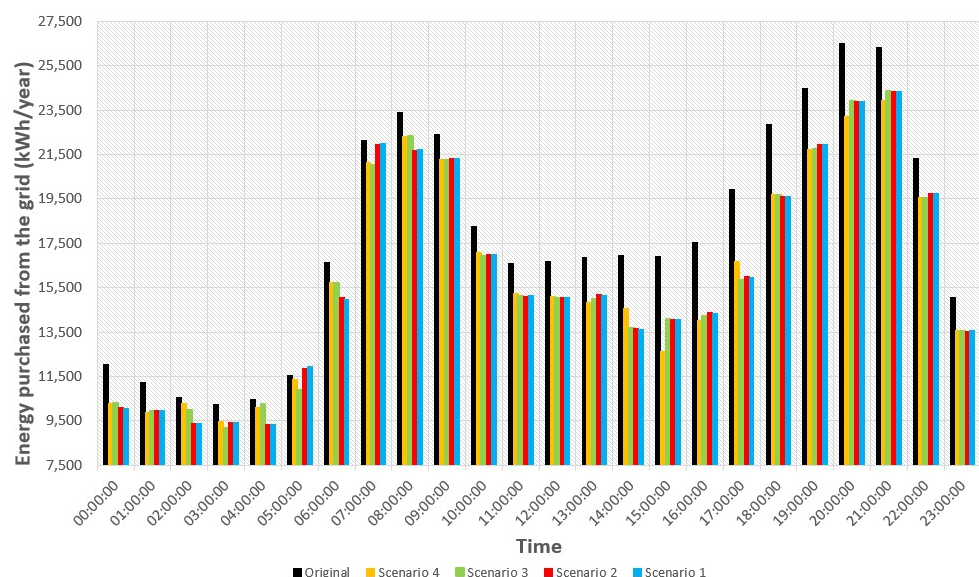


Figure 8. Energy purchased from the grid for the scenarios presented.

An economic analysis of the optimal solution for each scenario is performed to assess the feasibility of integrating wind and storage systems in the building. The optimal solution for each scenario is based on the lifespan of the adopted batteries. Therefore, it is necessary

to determine the amortization value of the annual investment and extend it to the lifespan of the turbine, which is 20 years. As shown in the graph in Figure 9, the balance sheet values are between approximately $-30,000$ EUR, corresponding to the initial investment of the project, and $80,000$ EUR, which represents the savings over the 20 years of the integration of the wind and storage project in the building. Therefore, it is quickly concluded that scenario 4 is the scenario with the highest profitability and that for the analysis period, it guarantees greater savings over the 20 years.

Scenario 1, which concerns the scenario where the battery lifespan is five years, is the worst performance regarding the speed of amortizing the investment made and total revenue for the period under analysis. Note that in the sixth year, there was practically no amortization due to the new investment in batteries, because after five years, the replacement of the batteries is necessary.

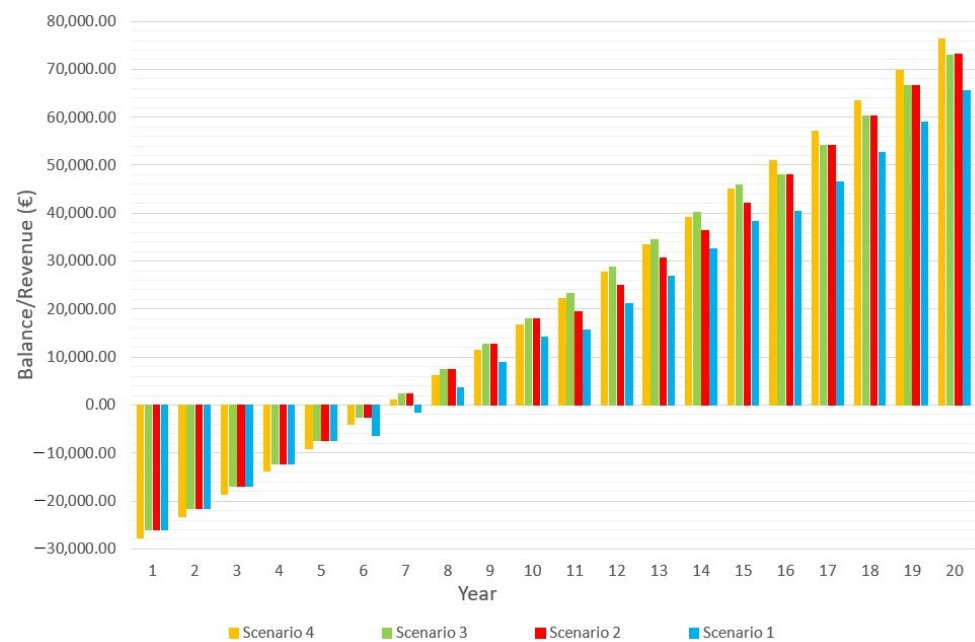


Figure 9. Monetary balance of investment for the different scenarios.

Focusing now on scenario 4, the main differences observed between it and the other scenarios are the adoption of a different ESS and the absence of reinvestment in the analysis period. Given that the adopted turbine and the energy tariff the same across the different scenarios, the notable difference between them is the use in terms of the maximum allowed cycles per year of the batteries, in this case, 300 cycles per year for a total of 6000. It was observed that the more cycles used per year, the greater the project's profitability per year. However, the savings will be fewer in the 20 years, due to the reinvestment in new ESS. This scenario, after 20 years, guarantees savings of 76,324.15 EUR, an amount sufficient for reinvestment in a new turbine and a new ESS, leaving around 44,000 EUR, because the investment in both adds up to an amount of 32,268.08 EUR.

Analysing the system's savings through local wind energy production and optimized energy storage, the balance sheet value for the twentieth year corresponds to 8.3% of the total energy and investment cost for that period.

4. Conclusions

The price of electricity generation using wind power systems is increasingly attractive when compared to traditional production plants. The installation of this type of electricity generation connected to the place of consumption itself, both in the low-voltage network and in the medium-voltage network, strongly facilitates a reduction in external energy dependence. For consumers, the benefits of installing small wind turbines and energy

storage systems generate tax benefits and reduced electricity bills, and a profitable system after the payback period.

The best location for installing wind turbines on the roof of the building was investigated. An analysis of the changes induced by the building itself, by the roof itself, and also by the nearby buildings was carried out. The airflow distortion from the nearby buildings was considered negligible by the difference in heights for the case study's building. The most favourable scenarios for the installation of the two types of available wind turbines were selected through CFD analysis. It was concluded that the two best scenarios are the installation of the Aeolos-H 20 kW turbine in the concrete block located relatively to the middle of the roof and one or more 10 kW Aeolos-V turbines at the north-facing ends of the roof.

The best scenario for integrating a self-consumption system based on the wind potential on the building under study was identified through the testing of the optimization model. Among all the options developed for the analysis of the model, the optimal one is scenario 4. This scenario consists of the installation of the Aeolos-H 20 kW turbine on the roof of the building, the tariff corresponds to the optional tariff, and the ESS is composed of a single-battery LG Resu with 12.4 kW. It guarantees an investment payback period of around 7 years, saving 76,324.15 EUR across the useful life of the system, and a 36% reduction in the consumption peaks in full hours and a reduction of around 42% for peak hours.

Author Contributions: Conceptualization, all authors; methodology, all authors; software, C.O.; validation, all authors; formal analysis, all authors; investigation, all authors; resources, all authors; data curation, C.O.; writing—original draft preparation, all authors; writing—review and editing, all authors; visualization, all authors; supervision, J.B. and A.C. All authors have read and agreed to the published version of the manuscript.

Funding: This work is financed by National Funds through the Portuguese funding agency, FCT—Fundação para a Ciência e a Tecnologia, within project LA/P/0063/2020.

Institutional Review Board Statement: Not applicable.

Informed Consent Statement: Not applicable.

Data Availability Statement: Data is contained within the article.

Conflicts of Interest: The authors declare no conflict of interest.

References

1. York, R.; Rosa, E.A.; Dietz, T. STIRPAT, IPAT and ImPACT: Analytic tools for unpacking the driving forces of environmental impacts. *Ecol. Econ.* **2003**, *46*, 351–365. [CrossRef]
2. Jones, D.W. How urbanization affects energy-use in developing countries. *Energy Policy* **1991**, *19*, 621–630. [CrossRef]
3. Al-Mulali, U.; Fereidouni, H.G.; Lee, J.Y.; Sab, C.N.B.C. Exploring the relationship between urbanization, energy consumption, and CO2 emission in MENA countries. *Renew. Sustain. Energy Rev.* **2013**, *23*, 107–112. [CrossRef]
4. European Union. Directive 2018/844 of the European Parliament and of the Council of 30 May 2018, amending Directive 2010/31/EU on the energy performance of buildings and Directive 2012/27/EU on energy efficiency. *Off. J. Eur. Union* **2018**, *L 156*, 75–91. Available online: <https://eur-lex.europa.eu/legal-content/EN/TXT/?uri=CELEX%3A32018L0844&qid=1628935298304> (accessed on 10 August 2022).
5. European Union. Directive 2018/2001 of the European Parliament and of the Council of 11 December 2018 on the promotion of the use of energy from renewable sources. *Off. J. Eur. Union* **2018**, *L 328/82*, 75. Available online: <https://eur-lex.europa.eu/legal-content/EN/TXT/PDF/?uri=CELEX:32018L2001&from=EN> (accessed on 10 August 2022)
6. Georgiou, G.; Nikolaidis, P.; Kalogirou, S.; Christodoulides, P. A Hybrid Optimization Approach for Autonomy Enhancement of Nearly-Zero-Energy Buildings Based on Battery Performance and Artificial Neural Networks. *Energies* **2020**, *13*, 3680. [CrossRef]
7. Filippidou, F.; Jimenez Navarro, J.; Pablo, J. *Achieving the Cost-Effective Energy Transformation of Europe's Buildings Energy Renovations via Combinations of Insulation and Heating & Cooling Technologies Methods and Data*; Publications Office of the European Union: Luxembourg, 2019. [CrossRef]
8. Palensky, P.; Dietrich, D. Demand Side Management: Demand Response, Intelligent Energy Systems, and Smart Loads. *IEEE Trans. Ind. Inform.* **2011**, *7*, 381–388. [CrossRef]

9. Georgiou, G.S.; Christodoulides, P.; Kalogirou, S.A. Real-time energy convex optimization, via electrical storage, in buildings—A review. *Renew. Energy* **2019**, *139*, 1355–1365. [[CrossRef](#)]
10. Walker, S.L. Building mounted wind turbines and their suitability for the urban scale—A review of methods of estimating urban wind resource. *Energy Build.* **2011**, *43*, 1852–1862. [[CrossRef](#)]
11. Chicco, G.; Mancarella, P. Distributed multi-generation: A comprehensive view. *Renew. Sustain. Energy Rev.* **2009**, *13*, 535–551. . [[CrossRef](#)]
12. Lu, L.; Ip, K.Y. Investigation on the feasibility and enhancement methods of wind power utilization in high-rise buildings of Hong Kong. *Renew. Sustain. Energy Rev.* **2009**, *13*, 450–461. [[CrossRef](#)]
13. El-Khattam, W.; Salama, M.M. Distributed generation technologies, definitions and benefits. *Electr. Power Syst. Res.* **2004**, *71*, 119–128. [[CrossRef](#)]
14. Balduzzi, F.; Bianchini, A.; Carnevale, E.A.; Ferrari, L.; Magnani, S. Feasibility analysis of a Darrieus vertical-axis wind turbine installation in the rooftop of a building. *Appl. Energy* **2012**, *97*, 921–929. [[CrossRef](#)]
15. Blackmore, P. *Siting Micro-Wind Turbines on House Roofs*, 1st ed.; IHS BRE Press: London, UK, 2008; p. 44.
16. Blackmore, P. *Building-Mounted Micro-Wind Turbines on High-Rise and Commercial Buildings*, 1st ed.; IHS BRE Press: London, UK, 2010.
17. Padoin, N.; Dal’Toé, A.T.; Rangel, L.P.; Ropelato, K.; Soares, C. Heat and mass transfer modeling for multicomponent multiphase flow with CFD. *Int. J. Heat Mass Transf.* **2014**, *73*, 239–249. [[CrossRef](#)]
18. Mangogna, A.; Valagussa, D.; Akintola, T.; Arietti, M.; Cicero, S.; Mordillo, F.; Pagani, A.; Sipione, R.; Corgnati, S. Towards nearly-zero energy buildings: HVAC system’s performances in the expected operative scenarios of Turin Energy Centre. In Proceedings of the REHVA Annual Conference “Advanced HVAC and Natural Gas Technologies”, Riga, Latvia, 6–9 May 2015; p. 8. [[CrossRef](#)]
19. Baños, R.; Manzano-Agugliaro, F.; Montoya, F.G.; Gil, C.; Alcayde, A.; Gómez, J. Optimization methods applied to renewable and sustainable energy: A review. *Renew. Sustain. Energy Rev.* **2011**, *15*, 1753–1766. [[CrossRef](#)]
20. Silva, P.C.; Almeida, M.; Bragança, L.; Mesquita, V. Development of prefabricated retrofit module towards nearly zero energy buildings. *Energy Build.* **2013**, *56*, 115–125. [[CrossRef](#)]
21. Turbine, A.W. Aeolos Wind Turbines Power Curves, United Kingdom. 2023. Available online: <https://www.windturbinestar.com/contact-us.html> (accessed on 24 January 2023).
22. Bergey, K.H. The Lanchester-Betz limit (energy conversion efficiency factor for windmills). *J. Energy* **1979**, *3*, 382–384. [[CrossRef](#)]
23. Jesus, B.; Cerveira, A.; Baptista, J. Optimization of Offshore Wind Farms Configuration Minimizing the Wake Effect. *Renew. Energy Power Qual. J.* **2022**, *20*, 30–36. [[CrossRef](#)]
24. Bianchini, A.; Gambuti, M.; Pellegrini, M.; Sacconi, C. Performance analysis and economic assessment of different photovoltaic technologies based on experimental measurements. *Renew. Energy* **2016**, *85*, 1–11. [[CrossRef](#)]

Disclaimer/Publisher’s Note: The statements, opinions and data contained in all publications are solely those of the individual author(s) and contributor(s) and not of MDPI and/or the editor(s). MDPI and/or the editor(s) disclaim responsibility for any injury to people or property resulting from any ideas, methods, instructions or products referred to in the content.